Chemistry
Europe
European Chemical
Societies Publishing

Efficient Synthesis of Monomeric Fe Species in Zeolite ZSM-5 for the Low-Temperature Oxidation of Methane

Tao Yu,[a, b] Yang Su,[a] Aiqin Wang,[a, c] Bert M. Weckhuysen,*[d] and Wenhao Luo*[a]

Direct oxidation of methane into value-added C1 oxygenated products, such as methanol, is essential and remains a significant challenge in the field of catalysis. In this work, we have prepared Fe/ZSM-5 materials via three different methods and investigated the influence of various preparation methods on the composition and catalytic performance of Fe/ZSM-5 for the low-temperature oxidation of methane. Through a combination of scanning transmission electron microscopy, ultraviolet-visible diffuse reflectance and ^{57}Fe Mössbauer spectroscopy, we have found that the highest proportion of monomeric Fe species of 71% could be achieved in the ZSM-5 zeolite by the solid-state ion-exchange method, affording an excellent C1 oxygenates yield of 120 mol/mol$_{Fe}$ with a C1 oxygenates selectivity of 96% at 50°C for 30 min in the aqueous solution of H_2O_2.

The forecasted availability and economical cost of methane, the principal component of natural gas and methane hydrates, require the development of efficient approaches for its transformation into value-added, easily transported commodity chemicals and liquid fuels.[1] The current industrial approach to utilizing methane is indirect and involves high-temperature and high-pressure oxidation to synthesis gas, which is subsequently transformed into methanol or to hydrocarbons via the well-known Fischer-Tropsch synthesis process.[2] Although the direct valorization of methane under low-temperature conditions is very attractive and more energy-efficient, transforming methane selectively to oxygenated species in one step poses

significant challenge, owing to the high stability of C–H bonds (i.e., 434 kJ/mol) in methane and the high reactivity of oxygenated products, such as methanol and formic acid, which can be easily overoxidized to CO_2 even at low conversion.[3]

In nature, the direct oxidation of methane into methanol can be realized under aerobic conditions with methane monooxygenase enzymes (MMOs) as biocatalytic catalysts using Fe and Cu as potential active metals.[4] Inspired by these enzymatic systems, researchers have tried to emulate similar enzyme-like active sites by using Fe- or Cu-containing zeolites in heterogeneous catalysts, to selectively activate methane under mild conditions.[5] Gas-phase systems using O_2,[6] N_2O,[7] H_2O[2b] as oxidants, as well as liquid-phase systems using H_2O_2[8] have been successfully developed in heterogeneous catalysis. Especially, of particular interest is the H_2O_2-based liquid-phase system, pioneered by the group of Hutchings,[5b] employing metal-containing zeolites as catalyst.

Recently, we have proposed that monomeric Fe species in Fe/ZSM-5 is the intrinsic active site for the low-temperature methane oxidation based on a combination of experimental and comprehensive (in situ) characterization investigations.[8b] Inevitably, the presence of disparate Fe species in different extent such as mononuclear, oligonuclear clusters and metal oxides particles are experimentally confirmed in heterogeneous Fe-containing zeolites,[9] and a majority of the Fe species shows limited activity as spectator species for the low-temperature methane oxidation.[10] Therefore, a deliberate increase in the portion of active species, monomeric Fe species in the Fe-containing zeolite, is highly desired in catalyst design, to improve the overall catalytical performance in methane oxidation.

In this work, we have compared three different synthesis methods, namely incipient wetness impregnation (IWI), liquid ion-exchange (IE) and solid-state ion-exchange (SSIE), to obtain Fe/ZSM-5 catalysts with a large portion of monomeric Fe species. The heterogeneous composition of disparate Fe species has been visualized and quantified by a combination of scanning transmission electron microscopy (STEM), ultraviolet-visible diffuse reflectance (UV-vis DR) and ^{57}Fe Mössbauer spectroscopy. The Fe/ZSM-5 prepared by the SSIE method, possesses the highest proportion (71%) of monomeric Fe species, affording a C1 oxygenates yield of 120 mol/mol$_{Fe}$ with a selectivity of 96% at 50°C for 30 min, reflecting, to the best of our knowledge, one of the highest values for metal-containing zeolites in methane oxidation under such benign conditions. Finally, additional insight into the reasons for the superior catalytic performance and successful maximization of the intrinsic active Fe species by the SSIE method is provided.

[a] T. Yu, Y. Su, Prof. Dr. A. Wang, Dr. W. Luo
CAS Key Laboratory of Science and Technology on Applied Catalysis
Dalian Institute of Chemical Physics, Chinese Academy of Sciences
457 Zhongshan Road, Dalian,
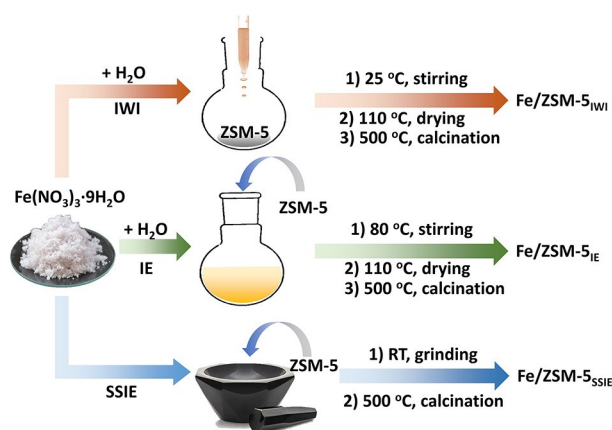116023 (P. R. China)
E-mail: w.luo@dicp.ac.cn

[b] T. Yu
University of Chinese Academy of Sciences
Beijing 100049 (P. R. China)

[c] Prof. Dr. A. Wang
State Key Laboratory of Catalysis
Dalian Institute of Chemical Physics,
Chinese Academy of Sciences
Dalian 116023 (P. R. China)

[d] Prof. Dr. B. M. Weckhuysen
Inorganic Chemistry and Catalysis group
Debye Institute for Nanomaterials Science
Utrecht University
Universiteitsweg 99, 3584 CG Utrecht (The Netherlands)
E-mail: B.M.Weckhuysen@uu.nl

ChemCatChem

Communications
doi.org/10.1002/cctc.202100299

**Chemistry
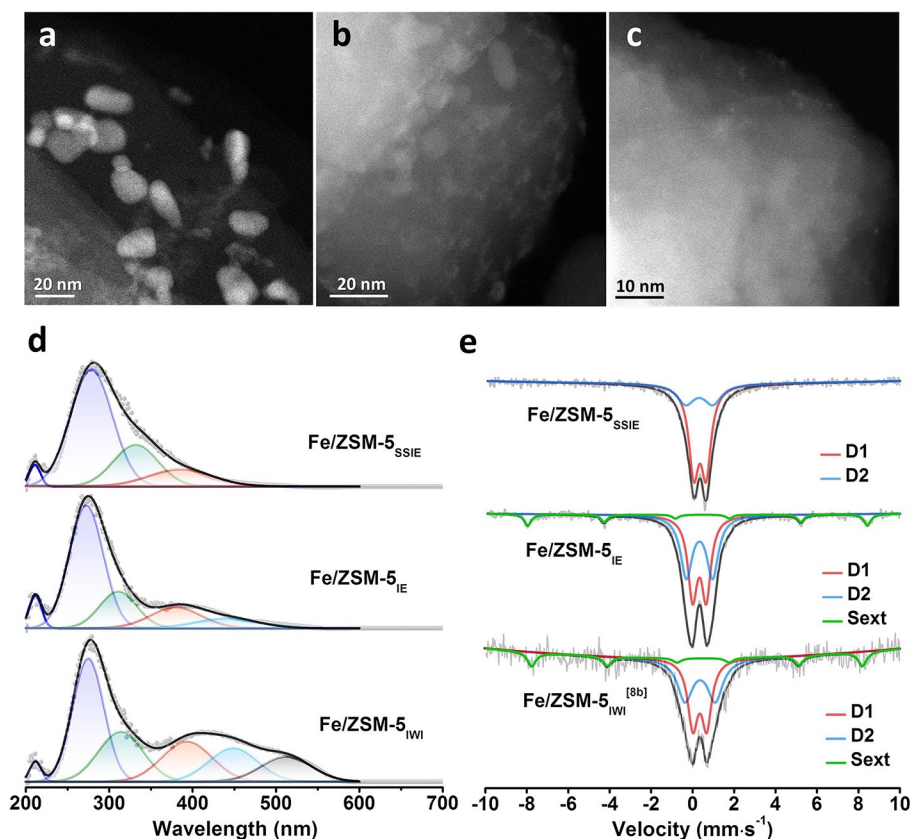Europe**
European Chemical
Societies Publishing

Three Fe/ZSM-5 catalysts with 0.5 wt% Fe loadings were prepared via the incipient wetness impregnation (IWI), ion-exchanged (IE) and solid-state ion-exchange (SSIE) methods and denoted as Fe/ZSM-5$_{IWI}$, Fe/ZSM-5$_{IE}$ and Fe/ZSM-5$_{SSIE}$, respectively. Iron (III) nitrate nonahydrate (Fe(NO$_3$)$_3$·9H$_2$O) and H-ZSM-5 (Si/Al = 13.5) powder were employed as metal precursor and support. The synthesis processes of the different catalysts are shown in Scheme 1, while details can be found in the

Supplementary Information. The corresponding metal content and N$_2$ physisorption analysis results are ~0.5 wt% (Table S1). All Fe/ZSM-5 samples show the same Fe/Al ratio of 0.06 and comparative surface area and porosity, indicating that different synthesis methods have limited impact on the physicochemical properties of the Fe/ZSM-5 catalysts. The X-ray diffraction (XRD) patterns of these Fe/ZSM-5 catalysts show only the typical reflections of the MFI zeolite structure, and no evidence of any other phase (Figure S1) was found, indicating the high dispersity of Fe species for all samples. In the STEM images of three Fe/ZSM-5 samples (Figure 1a–c), the Fe/ZSM-5$_{IWI}$ and Fe/ZSM-5$_{IE}$, exhibit a large number of Fe nanoparticles with a size of 5–25 nm observed on the external surface of zeolite. In contrast, no apparent Fe nanoparticles are observed for the Fe/ZSM-5$_{SSIE}$, indicating that the highly dispersed ultrasmall Fe species, likely located inside the zeolite ZSM-5 microporous structure.

UV-vis DR spectroscopy (Figure 1d) was conducted to further discriminate the different Fe species in the Fe/ZSM-5 catalysts. According to literature,[11] UV-vis DR spectra can differentiate Fe species into three categories: Monomeric Fe species with a wavelength of below 300 nm; small oligomeric Fe$_x$O$_y$ clusters with a wavelength of 300~400 nm; and Fe$_2$O$_3$ nanoparticles with a wavelength of above 400 nm. According to the above classification, the UV-vis DR spectra of these three Fe/ZSM-5 samples showed a strong signal at ~278 nm and a weak signal at ~210 nm, assigned to monomeric Fe^{3+} species

Scheme 1. Different preparation methods applied for synthesizing the Fe/ZSM-5 catalysts under study for the liquid-phase oxidation of methane.

Figure 1. (a–c) STEM images of Fe/ZSM-5$_{IWI}$, Fe/ZSM-5$_{IE}$ and Fe/ZSM-5$_{SSIE}$, respectively. (d) UV-vis DR spectra of Fe/ZSM-5$_{IWI}$, Fe/ZSM-5$_{IE}$ and Fe/ZSM-5$_{SSIE}$ catalysts. (e) ^{57}Fe Mössbauer spectra of Fe/ZSM-5$_{IWI}$,[8b] Fe/ZSM-5$_{IE}$ and Fe/ZSM-5$_{SSIE}$ catalysts.

ChemCatChem

Communications
doi.org/10.1002/cctc.202100299

**Chemistry
Europe**
European Chemical
Societies Publishing

Table 1. Comparison of catalytic performances for as-prepared catalysts and reported catalysts.

| Entry	Catalysts	Metal [wt%]	T [°C]	P [bar]	t [h]	Yield [mol/mol$_{Metal}$][a]	C1 oxygenates Sel. [%][b]	Ref.
1	Fe/ZSM-5$_{IWI}$	0.5	50	30	0.5	53	97	This work
2	Fe/ZSM-5$_{IE}$	0.5	50	30	0.5	70	98	This work
3	Fe/ZSM-5$_{SSIE}$	0.5	50	30	0.5	120	96	This work
4	Fe/ZSM-5	2.5	50	30.5	0.5	15.6	83	[5b]
5	CuFe/ZSM-5	2.5	50	30.5	0.5	15.7	85	[5b]
6	Fe/ZSM-5	0.5	50	30.5	0.5	37.8	86	[10]
7	FeN$_4$/GN	2.7	25	20	10	4.7	94	[13]
8	Fe-UiO-66	2.2	50	30	1	12	98	[14]
9	Rh/ZrO$_2$	0.3	70	30	1	1.3	78	[15]
10	Cr/TiO$_2$	1	50	30	20	57.9	93	[16]
11	AuPd/TiO$_2$	1	70	30.5	0.5	1.9	90	[17]
12	AuPd colloid	NA	50	35[c]	0.5	8.1	88	[18]

[a] Yield is defined as mole (C1 oxygenate products)/mole (active metal). [b] C1 Oxygenate selectivity, calculated as moles (oxygenates)/moles (produced) × 100%. [c] Reaction condition: 30 bar CH$_4$ and 5 bar O$_2$. NA: not available.

in octahedral and tetrahedral environment, respectively.[11b,c] Also, a signal at ~300–400 nm, indicative of oligomeric Fe$_x$O$_y$ clusters, was observed in all three samples. In addition, the absorption bands located above 400 nm, corresponding to the Fe$_2$O$_3$ nanoparticles, were observed in Fe/ZSM-5$_{IWI}$ and Fe/ZSM-5$_{IE}$ samples, but not in the Fe/ZSM-5$_{SSIE}$ sample, which is in good accordance with the observation by STEM. The spectra deconvolution results, which are shown in Figure 1d and Table S2, provide a semi-quantitative estimation of the distribution of the different Fe species. The proportion of mononuclear Fe species followed the order of Fe/ZSM-5$_{SSIE}$ > Fe/ZSM-5$_{IE}$ > Fe/ZSM-5$_{IWI}$.

^{57}Fe Mössbauer spectroscopy was further employed for the validation and quantification of different Fe species in the samples. The isomer shift (IS), quadrupole splitting (QS) and relative absorption area obtained by spectral deconvolution are listed in Table S3, which provide the valence state and coordination of different Fe species. As shown in Figure 1e, all Fe/ZSM-5 samples exhibit two doublets (D1 and D2) overlapping in the central region. The D1 components with the IS = 0.34~0.36 mm/s and QS = 0.60~0.70 mm/s are characteristic of Fe^{3+} in the octahedral coordination.[12] Combining the UV-vis DR results and the previously reported work,[8b] these components were assigned to the monomeric Fe^{3+} species. The D2 components with the IS = ~0.33–0.37 mm/s and QS = ~1.26–1.45 mm/s could be attributed to oligomeric Fe$_x$O$_y$ species (x ≥ 2) in the strongly distorted octahedral environment.[11a,12b] Moreover, the Fe/ZSM-5$_{IWI}$ and Fe/ZSM-5$_{IE}$ samples exhibit an evident sextet with the IS = 0.36 and QS = ~ −0.23–−0.29, indicative of bulk magnetic Fe$_2$O$_3$ particles.[9] These observations are again in an excellent agreement with the STEM and UV-vis DR results. Notably, the proportion of mononuclear Fe^{3+} species in the Fe/ZSM-5$_{SSIE}$ sample is estimated to be 71% (Table S3), which is a higher value than that found for Fe/ZSM-5$_{IWI}$ (i.e., 43%) and Fe/ZSM-5$_{IE}$ (i.e., 46%), indicating that the Fe/ZSM-5 sample obtained by SSIE possesses a higher portion of the monomeric Fe species than those prepared by the IWI and IE methods.

In a next stage of our study, the catalytic oxidation of methane was performed with three different Fe/ZSM-5 catalysts in the batch system at 50°C, with 30 bar of CH$_4$ and 0.5 M H$_2$O$_2$ aqueous solution. Four major products, including CH$_3$OH, CH$_3$OOH, HOCH$_2$OOH, and HCOOH, were detected and quantified by ^{1}H NMR (Figure S2 and Table S4). After a reaction time of 30 min, the Fe/ZSM-5$_{SSIE}$ sample (Table 1, entry 3) shows a C1 oxygenates yield of 120 mol/mol$_{Fe}$ with a C1 oxygenates selectivity of 96%, which was significantly higher than any other reported catalyst (Table 1). Interestingly, when evaluating the correlation between the yields of C1 oxygenated products and different Fe species, we have found that only the proportion of monomeric Fe species was positively correlated to the yield of different catalysts with a linear relationship (Figure 2). This agrees well with our previous work[8b] that monomeric Fe species were the intrinsic active sites for methane activation in the H$_2$O$_2$-based system. Thus, the superior catalytic performance of Fe/ZSM-5$_{SSIE}$ can be attributed to the presence of a higher proportion of monomeric Fe species compared with that in the Fe/ZSM-5$_{IWI}$ or Fe/ZSM-5$_{IE}$, as
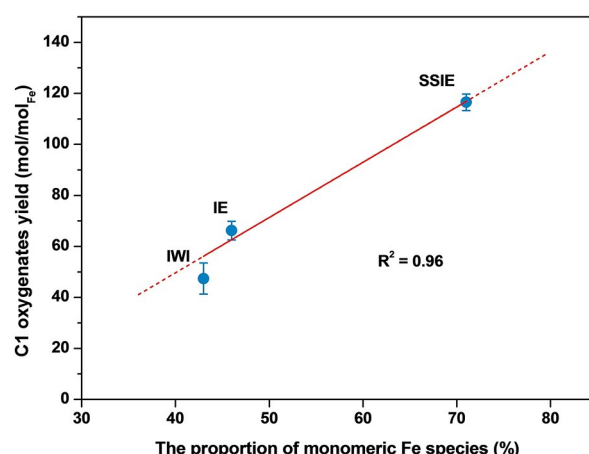

Figure 2. Correlation between the yield of C1 oxygenates and the relative proportion of monomeric Fe species quantified by ^{57}Fe Mössbauer spectroscopy. The line was added to guide the eye, but we are aware that the number of samples measured do not allow to provide more information from the data obtained.

confirmed by UV-vis DR (Figure 1d) and ^{57}Fe Mössbauer spectroscopy (Figure 1e).

Compared with the IE and IWI methods, the major difference for SSIE method is the avoidance of employing the solvent, in this case water, during the preparation of the catalyst materials. Therefore, employing water as solvent may play a key role in affecting the maximization of monomeric Fe species in the ZSM-5 during synthesis. To validate this hypothesis, UV-vis DR spectroscopy was performed to investigate the composition of different Fe^{3+} species presented in the precursor solution. As shown in Figure 3a, the spectrum of the aqueous solution of 0.043 M $Fe(NO_3)_3$ (the concentration used in the IWI method) shows one absorption signal at 447 nm, attributed to Fe^{3+} dimers formed from Fe^{3+} monomers.[19] This clearly demonstrates that dimeric Fe^{3+} complexes have been already formed in the precursor solution before the introduction into the ZSM-5 support. Combining with the UV-vis DR results and the previously reported work,[19,20] different $Fe(OH)(H_2O)_5^{2+}$, $Fe_2(OH)_2^{4+}$ and $Fe(OH)_2(H_2O)^{4+}$ species could be formed via hydrolysis under the employed IWI preparation conditions (i.e., pH = 1.74). The speciation distribution of different Fe^{3+} species for the 0.043 M $Fe(NO_3)_3$ solution can be calculated based on the pH value, as shown in Figure 3b (calculation details in the

Supporting Information), with the hydrated Fe^{3+} monomers $(Fe(H_2O)_6^{3+})$ and Fe^{3+} dimers $(Fe_2(OH)_2^{4+})$ as major species. Dimeric portions increase with pH at the expense of monomeric portions. The atomic percentage of such dimeric species in 0.043 M $Fe(NO_3)_3$ solution was determined to be ~17% in the precursor solution before impregnation. Therefore, the monomeric species start agglomeration in the precursor solution before impregnation. Although the dilute precursor solution employed for the IE method may alleviate the agglomeration of Fe species in the precursor solution (Figure S3), the followed drying process may cause an issue. After the drying process, the dehydrated samples for the Fe/ZSM-5$_{IWI}$ and Fe/ZSM-5$_{IE}$ appear clear absorption signals at >290 nm (Figure 3a and Figure S4), indicating the formation of oligomeric Fe species at a different extent before calcination, while the precursor for the zeolite Fe/ZSM-5$_{SSIE}$ material shows no observed absorption signals of oligomeric species in the UV-vis DR spectra. Additionally, the drying process, applied at 110 °C in both IWI and IE methods, could lead to an increase in the concentration of dimeric Fe^{3+} species in the precursor solution, which facilitates the formation of clusters and nanoparticles via hydrolysis (Figure S5). Finally, additional larger oligomers/bulk particles are inevitably formed by further agglomeration under the elevated temperature
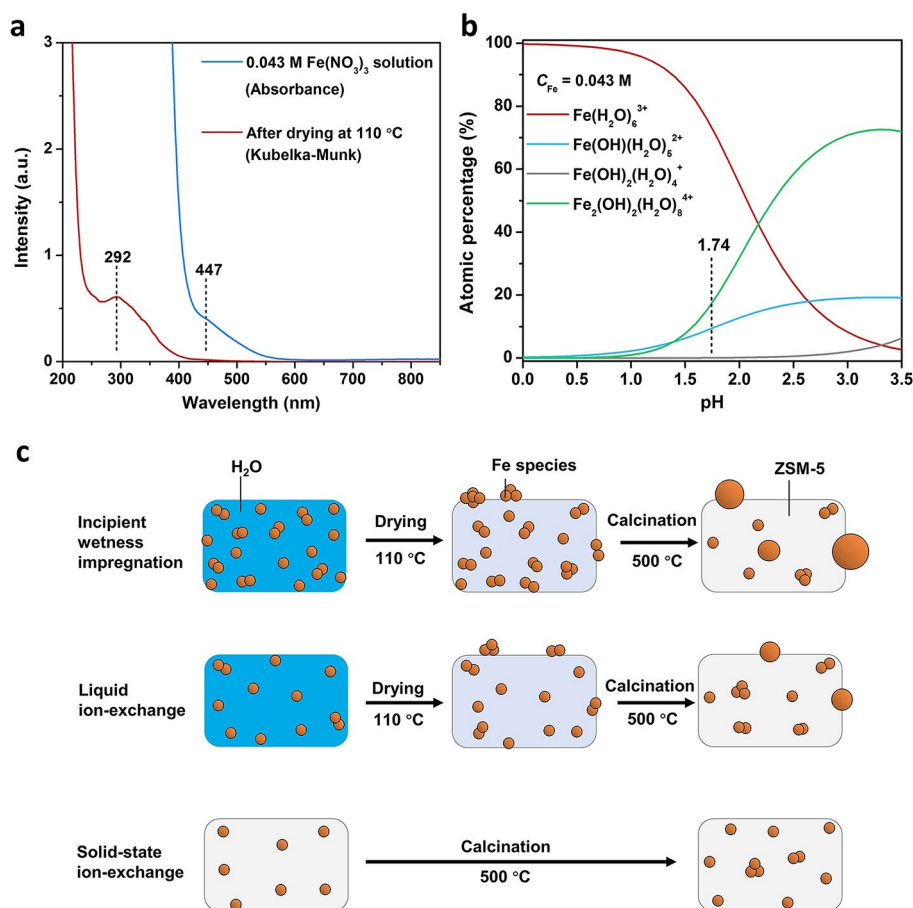
Figure 3. (a) UV-vis spectra of 0.043 M ferric iron nitrate solutions and the precursor of Fe/ZSM-5$_{IWI}$ after drying at 110 °C. (b) Fe^{3+} speciation distribution as a function of pH for 0.043 M ferric iron nitrate solutions based on the hydrolysis constants reported by Stefansson.[20] (c) The proposed evolutions of Fe species from the precursor to Fe/ZSM-5 by different methods.

during the subsequent calcination step for all the three samples under study, as observed in the STEM, UV-vis DR spectroscopy and ^{57}Fe Mössbauer spectroscopy data. Therefore, the use of water as solvent, employed in the IWI and IE methods, can inevitably result in the agglomeration of monomeric Fe species, in the precursor solution by hydrolysis and in the drying process (Figure 3c). Notably, the SSIE method could avoid those steps by the simplified synthetic process using no solvent, which efficiently inhibit the initial agglomeration of Fe species and formation of bulk Fe oxides species. The as-prepared Fe/ZSM-5$_{SSIE}$, enabling the maximization of the proportion of monomeric Fe species, affords an excellent catalytic performance for methane oxidation under mild conditions.

In summary, three methods including incipient wetness impregnation (IWI), liquid ion-exchange (IE) and solid-state ion-exchange (SSIE) were used to prepare Fe/ZSM-5 catalyst materials for the selective oxidation of methane. Our experimental results confirm that different preparation methods have a significant influence on the distribution of different Fe species in zeolite ZSM-5. The Fe/ZSM-5$_{SSIE}$ affords an excellent C1 oxygenates yield of 120 mol/mol$_{Fe}$, the highest to date, with a C1 oxygenates selectivity of 96% for the methane oxidation at 50 °C in the aqueous solution of H_2O_2. The SSIE method, employing no solvent, avoids the preparation of the precursor solution and drying process to remove the solvent, which could thus prevent the hydrolysis and subsequent agglomeration of Fe^{3+} monomers in the precursor solution and the drying process, enabling the as-prepared Fe/ZSM-5$_{SSIE}$ to possess the maximized proportion of the active monomeric Fe species. These findings provide valuable insights for the rational design of highly efficient metal-zeolite catalysts for the activation of methane as well as light alkanes under mild conditions.

Acknowledgements

Conflict of Interest

The authors declare no conflict of interest.

[1] a) B. G. Hashiguchi, M. M. Konnick, S. M. Bischof, S. J. Gustafson, D. Devarajan, N. Gunsalus, D. H. Ess, R. A. Periana, *Science* **2014**, *343*, 1232–1237; b) P. Schwach, X. Pan, X. Bao, *Chem. Rev.* **2017**, *117*, 8497–8520.

[2] a) J. H. Lunsford, *Catal. Today* **2000**, *63*, 165–174; b) V. L. Sushkevich, D. Palagin, M. Ranocchiari, J. A. Van Bokhoven, *Science* **2017**, *356*, 523–527.

[3] a) X. Meng, X. Cui, N. P. Rajan, L. Yu, D. Deng, X. Bao, *Chem* **2019**, *5*, 2296–2325; b) K. Ohkubo, K. Hirose, *Angew. Chem. Int. Ed.* **2018**, *57*, 2126–2129.

[4] a) C. E. Tinberg, S. J. Lippard, *Acc. Chem. Res.* **2011**, *44*, 280–288; b) R. Banerjee, Y. Proshlyakov, J. D. Lipscomb, D. A. Proshlyakov, *Nature* **2015**, *518*, 431–434; c) M. O. Ross, F. MacMillan, J. Wang, A. Nisthal, T. J. Lawton, B. D. Olafson, S. L. Mayo, A. C. Rosenzweig, B. M. Hoffman, *Science* **2019**, *364*, 566–570.

[5] a) A. R. Kulkarni, Z. J. Zhao, S. Siahrostami, J. K. Nørskov, F. Studt, *Catal. Sci. Technol.* **2018**, *8*, 114–123; b) C. Hammond, M. M. Forde, M. H. Ab Rahim, A. Thetford, Q. He, R. L. Jenkins, N. Dimitratos, J. A. Lopez-Sanchez, N. F. Dummer, D. M. Murphy, A. F. Carley, S. H. Taylor, D. J. Willock, E. E. Stangland, J. Kang, H. Hagen, C. J. Kiely, G. J. Hutchings, *Angew. Chem. Int. Ed.* **2012**, *51*, 5129–5133; c) K. T. Dinh, M. M. Sullivan, P. Serna, R. J. Meyer, M. Dincă, Y. Román-Leshkov, *ACS Catal.* **2018**, *8*, 8306–8313.

[6] a) S. Grundner, M. A. C. Markovits, G. Li, M. Tromp, E. A. Pidko, E. J. M. Hensen, A. Jentys, M. Sanchez-Sanchez, J. A. Lercher, *Nat. Commun.* **2015**, *6*, 7546; b) K. T. Dinh, M. M. Sullivan, K. Narsimhan, P. Serna, R. J. Meyer, M. Dincă, Y. Román-Leshkov, *J. Am. Chem. Soc.* **2019**, *141*, 11641–11650.

[7] a) E. V. Starokon, M. V. Parfenov, S. S. Arzumanov, L. V. Pirutko, A. G. Stepanov, G. I. Panov, *J. Catal.* **2013**, *300*, 47–54; b) B. E. R. Snyder, P. Vanelderen, M. L. Bols, S. D. Hallaert, L. H. Böttger, L. Ungur, K. Pierloot, R. A. Schoonheydt, B. F. Sels, E. I. Solomon, *Nature* **2016**, *536*, 317–321.

[8] a) S. Bai, F. Liu, B. Huang, F. Li, H. Lin, T. Wu, M. Sun, J. Wu, Q. Shao, Y. Xu, X. Huang, *Nat. Commun.* **2020**, *11*, 954; b) T. Yu, Z. Li, W. Jones, Y. Liu, Q. He, W. Song, P. Du, B. Yang, H. An, D. M. Farmer, C. Qiu, A. Wang, B. M. Weckhuysen, A. M. Beale, W. Luo, *Chem. Sci.* **2021**, *12*, 3152–3160.

[9] P. F. Xie, Y. J. Luo, Z. Ma, C. Y. Huang, C. X. Miao, Y. H. Yue, W. M. Hua, Z. Gao, *J. Catal.* **2015**, *330*, 311–322.

[10] C. Hammond, N. Dimitratos, R. L. Jenkins, J. A. Lopez-Sanchez, S. A. Kondrat, M. Hasbi ab Rahim, M. M. Forde, A. Thetford, S. H. Taylor, H. Hagen, E. E. Stangland, J. H. Kang, J. M. Moulijn, D. J. Willock, G. J. Hutchings, *ACS Catal.* **2013**, *3*, 689–699.

[11] a) J. Y. Wang, H. A. Xia, X. H. Ju, Z. C. Feng, F. T. Fan, C. Li, *J. Catal.* **2013**, *300*, 251–259; b) M. Schwidder, M. S. Kumar, K. Klementiev, M. M. Pohl, A. Brückner, W. Grünert, *J. Catal.* **2005**, *231*, 314–330; c) J. Pérez-Ramírez, J. C. Groen, A. Brückner, M. S. Kumar, U. Bentrup, M. N. Debbagh, L. A. Villaescusa, *J. Catal.* **2005**, *232*, 318–334.

[12] a) M. Iwasaki, K. Yamazaki, K. Banno, H. Shinjoh, *J. Catal.* **2008**, *260*, 205–216; b) G. I. Panov, A. A. Shteinman, K. A. Dubkov, N. S. Ovanesyan, E. V. Starokon, *J. Catal.* **2002**, *207*, 341–352.

[13] X. Cui, H. Li, Y. Wang, Y. Hu, L. Hua, H. Li, X. Han, Q. Liu, F. Yang, L. He, X. Chen, Q. Li, J. Xiao, D. Deng, X. Bao, *Chem* **2018**, *4*, 1902–1910.

[14] W. Zhao, Y. Shi, Y. Jiang, X. Zhang, C. Long, P. An, Y. Zhu, S. Shao, Z. Yan, G. Li, Z. Tang, *Angew. Chem. Int. Ed.* **2021**, *60*, 5811–5815.

[15] Y. Kwon, T. Y. Kim, G. Kwon, J. Yi, H. Lee, *J. Am. Chem. Soc.* **2017**, *139*, 17694–17699.

[16] Q. Shen, C. Cao, R. Huang, L. Zhu, X. Zhou, Q. Zhang, L. Gu, W. Song, *Angew. Chem. Int. Ed.* **2020**, *59*, 1216–1219.

[17] C. Williams, J. H. Carter, N. F. Dummer, Y. K. Chow, D. J. Morgan, S. Yacob, P. Serna, D. J. Willock, R. J. Meyer, S. H. Taylor, G. J. Hutchings, *ACS Catal.* **2018**, *8*, 2567–2576.

[18] N. Agarwal, S. J. Freakley, R. U. McVicker, S. M. Althahban, N. Dimitratos, Q. He, D. J. Morgan, R. L. Jenkins, D. J. Willock, S. H. Taylor, C. J. Kiely, G. J. Hutchings, *Science* **2017**, *358*, 223–227.

[19] M. Zhu, B. W. Puls, C. Frandsen, J. D. Kubicki, H. Zhang, G. A. Waychunas, *Inorg. Chem.* **2013**, *52*, 6788–6797.

[20] A. Stefánsson, *Environ. Sci. Technol.* **2007**, *41*, 6117–6123.